Progress in Medical Devices
ISSN: 2957-5478

Zentime

Research Article https://doi.org/10.61189/434505lacrsk

An investigation of upper extremity impedance modeling and sensory thresholds in envelope wave electrical stimulation

Renling Zou[1], Yuhao Liu[1], Yicai Wu[1], Liang Zhao[1], Jigao Dai[1], Xiufang Hu[1], Xuezhi Yin[2]

[1]School of Health Sciences and Engineering, University of Shanghai for Science and Technology, Shanghai, 200000, China. [2]Shanghai Berry Electronic Technology Co., Ltd., Shanghai, 200000, China.

Corresponding authors: Renling Zou.

Acknowledgement: This work was supported by Science and Technology Commission of Shanghai Municipality (21S31906000), the National Natural Science Foundation of China (NSFC) Grant (61803265), and Medical-industrial cross-project of USST Grant (1022308524).

Declaration of conflict of interest: None.

Received April 24, 2024; Accepted June 25, 2024; Published December 31, 2024

Highlights

- This study introduces a novel impedance model for the human upper limb, providing a highly accurate fit between frequency and impedance values.
- The newly proposed Voltage Perception Threshold (VPT) method offers a more reliable measure of electrical stimulus sensation, independent of current magnitude and output frequency, compared to the traditional Current Perception Threshold (CPT).

Abstract

Objectives: To investigate how impedance values and sensory thresholds at various human upper limb sites affect the parameter settings of electrical stimulation equipment in low and medium frequency envelope electrical stimulation therapy. **Methods:** The study involved testing different upper limb sites on 22 healthy subjects (ages 21-25, 11 males and 11 females) by adjusting the modulation wave frequency, carrier frequency, and current intensity of the output. Five types of electrodes of various sizes were used in the tests. **Results:** The impedance test results for the human upper limb showed a wide range of impedance values across electrodes of different sizes. A new impedance model of the human upper limb was proposed, which accurately fits the relationship between frequency and impedance values. In electrical stimulus sensory experiments, the voltage perception threshold (VPT) introduced in this study was identified as a novel metric for electrical stimulus sensation. Unlike the current perception threshold, VPT does not consider the effects of current magnitude and output frequency. The range of sensory thresholds was 6-8 V, while the suprathreshold was 9-11 V. Neither experiment showed gender differences. **Conclusions:** Determining the value of the power supply and the output intensity of device power amplification circuitry based on the VPT can provide a more precise therapeutic dose for electrical stimulation therapy.

Keywords: Electrical stimulation, human impedance, voltage perception threshold, envelope

Introduction

As a rehabilitation technique for neurological injury diseases, electrical stimulation therapy has garnered extensive attention and research in recent years due to its ability to help patients rebuild or restore some motor functions [1, 2]. Currently, various forms of electrical stimulation instruments are available on the market. Most of these devices adjust treatment intensity based on subjective pain perception of patients, lacking capability to record the physiological information, such as bioimpedance, surface electromyography [3]. This kind of physiological information is essential for guiding role in the treatment of patients [4-7].

Address correspondence to: Renling Zou, School of Health Sciences and Engineering, University of Shanghai for Science and Technology, No.516 Jungong Road, Shanghai 200000, China. E-mail: zourenling@usst.edu.cn.

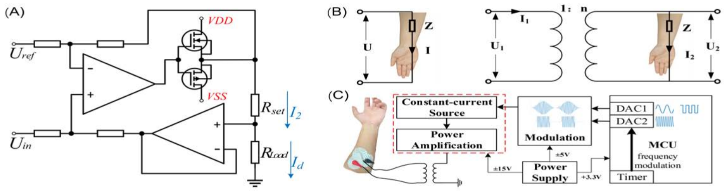

Figure 1. Electrical stimulation circuit block diagram. (A) Constant-current source model of the electrical stimulation device; (B) Functional block diagram of electrical stimulation module; (C) The relationship between the impedance of human body and the power supply of power amplifier circuit. VDD,voltage drain drain; VSS,voltage source and sink; DAC,digital-to-analog converter; MCU,microcontroller unit.

The electrical model of the human body is highly complex, and the biological passive impedance model contains complex domains, necessitating the consideration of both direct current and alternating current in waveform selection [8-12]. YinQimin noted an issue when comparing square waves with differential waves in experiments: square waves induce the human body to produce differential waves, making it impossible to evaluate the effect of the two waveforms by comparing two different differential waves [13-15]. One key point we propose is that a patient's sensation to a stimulus does not necessarily indicate that the waveform is undistorted. Many studies lack the measurement of relevant physiological information before setting electrical stimulation parameters [15]. Zhou et al. did not account for measuring human body impedance before designing the boost voltage source [16]. Boosting the power supply to a certain value without determining the impedance value can lead to excessive circuit power consumption or cause output waveform distortion in electrical stimulation equipment.

Pain and tolerance threshold can also be considered as a form of physiological information, providing valuable clinical insights for evaluating neurological defects, selecting appropriate treatments, and monitoring sensory recovery after injury [17]. Electrical stimulation is a simple method for measuring pain sensation [17-20]. Previous studies have predominantly used current perception threshold (CPT) as a criterion [21-25]. Hiremath SV et al. showed that the receptive intensity increases with the higher pulse amplitude and frequency [26]. However, there is limited research on the reasons for the differences in CPT across different genders and ages. This is because the adjustment of electrical stimulation intensity is usually based on subjective verbal feedback, and information about the stimulation waveform, electrode size and other parameters is often incomplete or inconsistent. Thus, relying on a patient's subjective experience to determine stimulation dose is unreliable, highlighting the need for methods to objectively quantify pain. Seno SI et al. measured CPT with five electrode sizes, finding that the CPT values increased with electrode size [18]. After adjusting for body fat percentage or body water content, the logarithmic conversion values showed no gender differences between electrode pairs.

The impedance value of the human upper limb directly affects the supply voltage required by stimulation equipment, while the sensory threshold affects the parameter setting of the electrical stimulation and the therapeutic effect. This study was conducted to investigate the influence of human upper limb impedance and electrical stimulation sensory threshold on the parameter setting of electrical stimulation equipment using a controlled variable method to obtain relevant physiological information. The variables examined included five different sizes of hydrogel electrodes, modulating waveforms ranging from 2-150 Hz, carrier waveforms with output frequencies from 1-10 kHz, and output currents ranging from 0-20 mA.

Methods and materials

Theory background

Figure 1A illustrates a model of a constant current source circuit used in electrical stimulation equipment. The current magnitude is given by (1):

$$I_d = I_2 = \frac{U_{in}}{R_{set}} \tag{1}$$

where I_d represents the current flowing through the human body (with R_{Load} as the impedance of the human upper limb), U_{in} is the input voltage signal, and VDD (voltage drain drain) is the power supply for the power amplifier circuit in the device. U_{ref} is referenced to ground, the output current is solely determined by the input voltage U_{in}, and is independent of the load impedance R_{Load}.

The relationship between the power supply of the power amplifier module and the impedance amplitude of the human body can be simplified to the model shown in **Figure 1B**. Previous studies have shown that the intensity of electrical stimulation is typically determined by the current magnitude [27]. When the output current *I* is fixed, the power supply voltage *U* should be set according to the maximum impedance *Z*. If $U < Z * I$, the output waveform will be distorted; if *U* is too large, it will increase the power consumption of the entire circuit. Therefore, before setting the power supply value, it is crucial to determine the range of the human impedance values. To prevent the output waveform distortion or excessive *U* values during the measurement, this study first measured the human impedance using the circuit shown in **Figure 1B**. A transformer was added between the constant-current source power amplifier circuit and the human body load. The transformer isolates the human body from the circuit board and acts as an impedance transformer. By converting the high impedance on the load side to a lower impedance on the output side, a lower supply voltage can be utilized without increasing circuit power consumption. In this study, the power supply *U1* was set to 15 V, and the number of turns on the transformer's secondary coil was chosen to be 20, allowing for a maximum undistorted voltage of 300 V to be measured on the load side of the human body. The power supply voltage can be adjusted at a later stage according to the measured impedance values.

Instrument design

This device utilizes a constant-current source for the electrical stimulation output, ensuring that the output current remains unaffected by changes in the impedance of the human upper limb. **Figure 1C** presents a functional block diagram of the electrical stimulation module, including MCU (microcontroller unit), modulation module, constant-current source output and power amplification modules. The DAC1 (digital-to-analog converter) output of the MCU provides the modulating waveform, which can be selected as either a sinusoidal waveform or square waveform. Given the complex impedance characteristics of the human body, a square wave output will result in a differential wave, so DAC2 is configured to output only alternating current signals. The waveform frequency can be modulated by adjusting the timer settings. To enhance bandwidth capacity, the outputs from the MCU's two DACs are followed by a voltage follower. It is necessary to convert the DAC1 output to 0-1 V and the DAC2 output to -1 -1 V. These outputs are then fed into the AD835 multiplier, where they are modulated to produce the two waveforms depicted in the modulation module. Finally, the electrical stimulation is delivered to the human body through electrode pads via a constant current source and power amplification circuit.

Before conducting the experiment, it is essential to evaluate the output capability of the constant current source. This evaluation was performed using a 100 Hz sinusoidal modulating waveform and a 2 kHz sinusoidal carrier waveform while outputting a constant current. The voltage across the resistive loads, with varying resistance values, was measured. The output current strength was set in increments ranging from 5 to 25 mA, divided into 5 steps. The nominal resistance value of the loads were between 1 and 5 KΩ (with a power rating of 50W and an accuracy of 1%), and each load was measured individually. **Table 1** presents the measurement results, including the average value and standard deviations. The maximum standard deviation observed was 0.17 mA, which basically meets the requirements for a constant current source.

Results

The experiment used five hydrogel electrode pads in different sizes, as shown in **Figure 2**, to perform the following two tests: 1) A fixed current was output, while the modulating wave frequency and carrier frequency were adjusted. The impedance value of different upper limb sites was then determined using Ohm's law by measuring the voltage at various points on the upper limb. 2) Currents of varying sizes and frequencies were output to quantify the pain perception threshold. The study involved 11 healthy male subjects (age: 23±2 years, height: 173.2±5.1 cm, weight: 70.8±13.2 Kg) and 11 healthy female subjects (age: 22±2 years, height: 163±4.7 cm, weight: 52±8.6 Kg). All subjects participated voluntarily and were informed of the purpose of the experiment. They were also made aware that they could withdraw from the experiment at any time.

Human Upper Limb Impedance Measurement

The measurement of human upper limb impedance considered several factors: different parts of the human upper limb, modulating wave frequency, carrier frequency and electrode size. As shown in **Figure 3**, the positive electrode of the differential electrode pair was fixed on the left brachioradialis muscle, and the negative elec-

Table 1. Output current corresponding to different resistance loads and their average value and SD

		Current intensity / mA				
		5	10	15	20	25
Load/Ω	1K	5.10	10.8	15.20	20.40	25.40
	2K	5.15	10.2	15.00	20.20	25.20
	3K	5.00	9.98	14.96	19.96	24.88
	4K	4.10	10.10	15.10	20.10	25.12
	5K	5.08	10.20	15.20	20.28	25.26
Statistics	mv	5.08	10.18	15.09	20.19	25.17
	sd	0.05	0.14	0.10	0.15	0.17

Note: MV, mean value; SD, standard deviation.

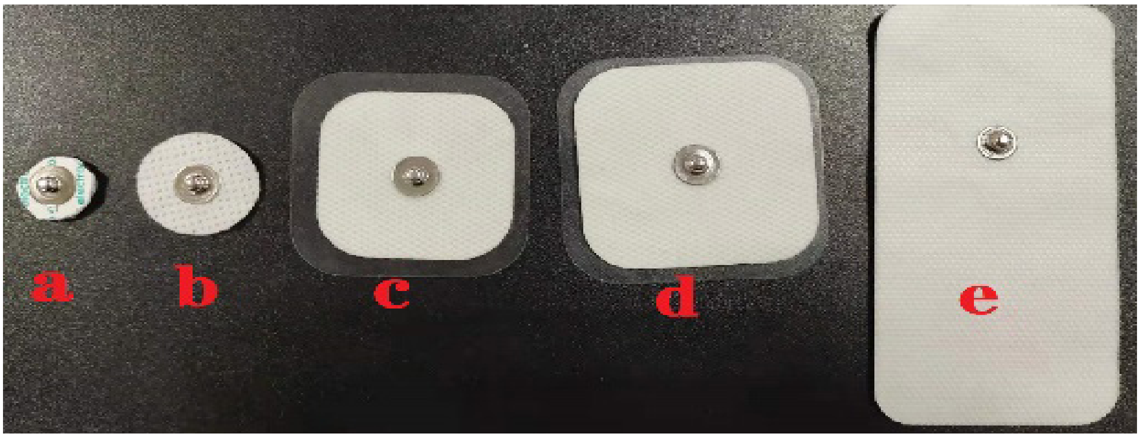

Figure 2. Hydrogel electrode size. The size of each electrode sheet: 3.53cm^2 (a), 9.82cm^2 (b), 16 cm^2 (c), 25 cm^2 (d), 50 cm^2 (e).

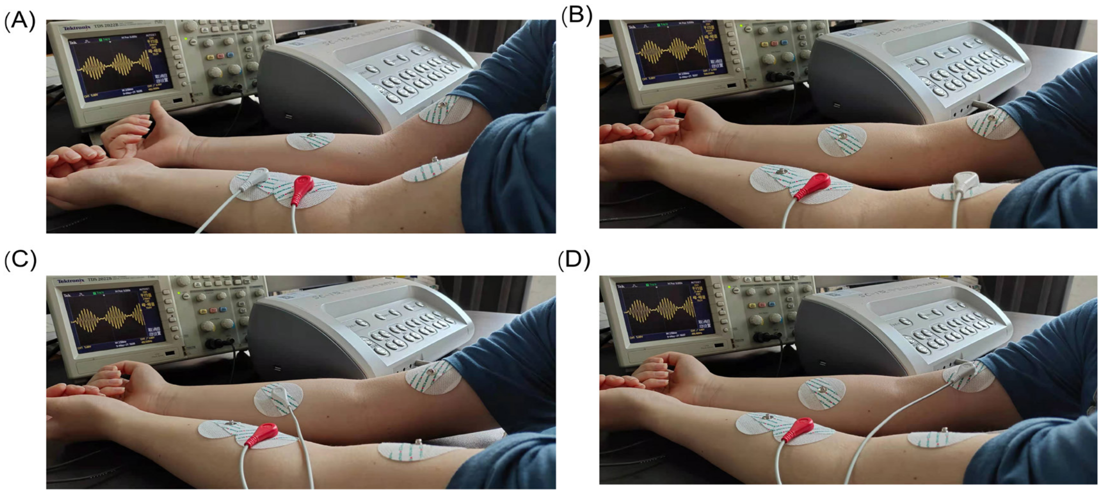

Figure 3. Impedance measurements were performed on different positions of the upper limb. (A) left brachioradialis-left brachioradialis; (B) left brachioradialis-left biceps brachii; (C) left brachioradialis-right brachioradialis; (D) left brachioradialis-right biceps brachii.

trode was placed on the following four different sites: (A) left brachioradialis muscle, (B) left biceps brachii muscle, (C) right brachioradialis muscle, and (D) right biceps brachii muscle. The electrodes used were Ag/AgCl disposable cardiac electrode sheets. The modulating waveform was a 10 Hz sine wave, and the carrier waveform was a 1000 Hz sine wave. During the experiment, the modulating wave frequency was varied in 1 Hz increments within the range of 2-150 Hz, with results consistently around 19.2 V. This consistency indicates that varying the electrode position on the upper limb or changing the modulating wave frequency had negligible effects on the measured impedance values. Consequently, this experiment primarily focused on examining the relationship between carrier frequency, electrode size, and the impedance of the upper limb.

Measurement result

Table 2. The impedance minima, maxima, and peak frequencies corresponding to the impedance maxima measured for the two test groups in the carrier frequency range of 100-10000 Hz (standard deviation in parentheses)

Electrode (cm^2)	Male (n=11)					Female (n=11)				
	3.53	9.82	16	25	50	3.53	9.82	16	25	50
Min/KΩ	0.51 (0.05)	0.45 (0.04)	0.39 (0.04)	0.34 (0.05)	0.27 (0.02)	0.51 (0.04)	0.44 (0.03)	0.42 (0.03)	0.38 (0.04)	0.31 (0.02)
Max/KΩ	21.80 (3.52)	10.98 (3.53)	8.06 (0.89)	6.18 (0.56)	3.79 (0.32)	19.80 (3.18)	11.68 (2.82)	8.16 (0.79)	5.56 (0.57)	3.29 (0.29)
Peak frequency/ Hz	2000	1500	700	500	400	2000	1500	700	500	400

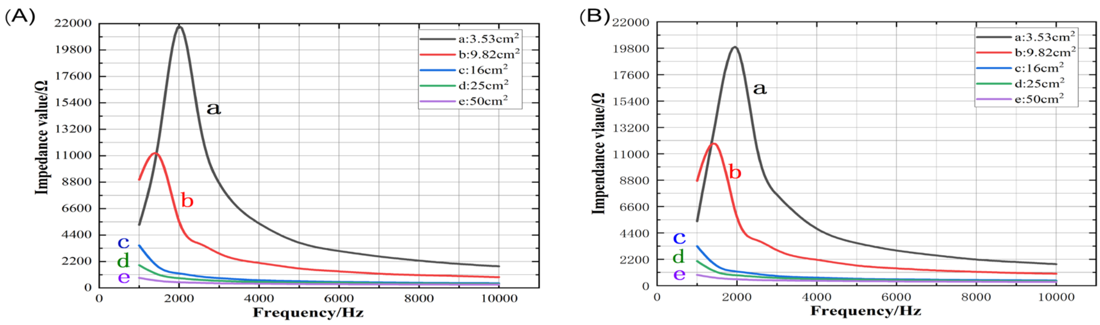

Figure 4. Carrier frequency (100-10000 Hz) corresponded impedance value of five electrode sizes. (A) Male subjects; (B) Female subjects.Increments of 100 Hz within the 100-1000 Hz range, 500 Hz within 1-3 kHz range, and 1000 Hz for adjustments within 3-10 kHz range.

The carrier frequency was adjusted in increments of 100 Hz within the 100-1000 Hz range, 500 Hz within 1-3 kHz range, and 1000 Hz for adjustments within 3 -10 kHz range. Measurements were made sequentially using five electrode pads. Tests were conducted separately on 11 males and 11 female subjects. **Figure 4A** shows the test results for the male group, and **Figure 4B** shows the test results for the female group. The data indicate that the impedance values varied significantly with different electrode sizes, although the overall trend remained consistent. As the carrier frequency increased, the impedance initially peaked before decreasing as the frequency continued to rise. Additionally, larger electrode sizes corresponded to lower carrier frequencies at which peak impedance occurred. When the carrier frequency exceeded 5 kHz, the impedance plateaued. No significant differences were observed between genders. **Table 2** lists the three impedances for both test groups: the impedance minima, maxima, and peak frequencies corresponding to the impedance maxima measured for each electrode size. The peak frequencies were identical, and the impedance values did not differ significantly by gender.

Human Upper Limb Impedance Model

Analysis of the experimental data reveals a maximum impedance peak at a specific frequency [28]. The three-element equivalent circuit model proposed by Cole is widely used in analyzing human impedance. In an RC (Resistance-capacitance) circuit model, impedance peaks are not possible; therefore, the traditional human impedance model is not suitable for electrical stimulation involving the envelope waveform formed by modulating and carrier waveforms. For low- and medium- frequency envelope waveform electric stimulation, a suitable passive circuit model can be used to fit the data, and the values of the parameters related to the impedance of the upper limb of the human body can be further analyzed. Based on the impedance variation pattern of the human upper limb shown in **Figure 5**, it is suggested that the upper limb exhibits not only capacitive characteristics but also possibly inductive characteristics. The combination of inductance and capacitance may result in a resonance frequency where the impedance peaks. The expression for the impedance value *Z* is:

$$Z = R_1 + \frac{1}{j\omega C} // (R_2 + j\omega L) = R_1 + \frac{\frac{1}{j\omega C}(R_2 + j\omega L)}{j\omega L + R_2 + \frac{1}{j\omega C}} \quad (2)$$

To achieve a peak frequency in this model, assuming , the expression of *Z* is:

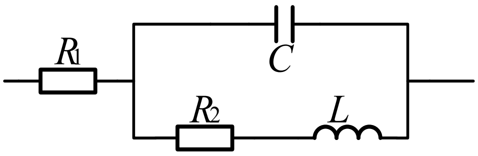

Figure 5. Passive circuit model of human impedance.

$$Z \approx R_1 + \frac{\frac{L}{C}}{R_2 + j(\omega L - \frac{1}{\omega C})} \quad (3)$$

When $\omega L = \frac{1}{\omega C}$, the impedance value Z reached its maximum, and the maximum value $z_m \approx L/(R_2C)$. The corresponding peak frequency $z_m \approx L/(R_2C)$. **Table 3** presents the relevant data measured in the experiment.

Figure 6 shows the fitting result of formula (3) to the impedance value and its corresponding frequency. Twenty-one discrete points were obtained from each electrode, with the solid line representing the fitted curve. **Table 4** shows the fitted values of the components in the circuit model and the theoretical peak frequencies and maxima impedance calculated from the fitted values. The analysis reveals that the inductance L remains nearly constant, while the fitted capacitance C increases with electrode size, and the fitted resistance R_2 decreases with electrode size. A linear relationship was observed between electrode area (Area), capacitance C, and resistance R_2. The relationship between C and electrode size (Area) is defined by equation (4) and the relationship between R_2 and C is defined by equation (5). Based on the fitted values, the peak frequency calculated by the formula $f_{peak}=1/(2\pi\sqrt{LC})$ closely matches the original measured peak frequency. Similarly, the theoretical impedance value calculated by $z_m \approx L/(R_2C)$ is consistent with the measured value. In summary, the circuit model accurately fits to the measured impedance of the human upper limb, providing a robust model for obtaining various physiological information in medical research involving low and medium frequency envelope electrical stimulation.

$$C = 5.577Area - 18.15 \quad (4)$$

$$R_2 = \frac{10000}{\sqrt{C}} \quad (5)$$

Pain perception threshold measurement

The relationship between pain perception, current intensity, and carrier frequency was investigated by adjusting these variables during experiments conducted with five electrodes of different sizes. Pain perception was assessed based on patient feedback, where the current intensity and carrier frequency were varied, and the patient's reactions were observed. When electrical stimulation was present, adjustments were made until the sensation disappeared, though current output remained—this point was recorded as the subsensory threshold. The sensory threshold was recorded when electrical stimulation was felt, and the supra-sensory threshold was recorded when there was noticeable electrical stimulation and numbness [29].

According to these three sensory criteria, the carrier frequency was adjusted within the 6-10 kHz, where the impedance changes slowly. The current intensity was varied from 0-20 mA, with a increment about 1 mA.

During measurement, as the carrier frequency increased, the voltage amplitude decreased, resulting in reduced electrical stimulation experienced by the subjects. Increasing the current at this point raised the voltage amplitude and enhanced the electrical stimulation. **Table 5** shows the test results for one subject. For each type of electrode, the standard deviation of the voltage measured at the three sensation levels was less than 1V across different frequencies. The results indicated consistent voltage thresholds for electrical stimulation among subjects. In summary, the voltage at both ends of the stimulation site can replace CPT as a measure of pain perception, namely voltage perception threshold (VPT).

Figure 7 shows the VPT values obtained from each electrode, separated by sex. **Figure 7a** shows the perceptual threshold corresponding to the five electrodes. The measured sensory threshold values for males were 11.04, 9.20, 6.97, 7.17 and 6.92 V, while the values for females were 12.75, 9.25, 6.68, 7.13 and 6.15 V, respectively. There were significant differences between sexes when using 3.53 cm^2 ($P < 0.001$) and 50 cm^2 ($P < 0.01$) electrodes, while the VPT values were similar for other three electrodes. Figure 7b shows the measurement results above the sensory threshold. The measured supra-sensory threshold values for males were 16.54, 11.36, 8.49, 8.89, and 8.51 V, whereas for females, the values were 18.58, 12.74, 8.61, 9.12, and 8.17 V. Significant differences between males and females were found when using the 3.53 cm^2 ($P < 0.001$) and 9.82 cm^2 ($P < 0.001$) electrodes, while VPT values remained consistent for the other three electrodes. For both sensory and supra-sensory

Table 3. Human body impedance obtained from five electrodes

Electrode	Z_{min}/KΩ	Z_{max}/KΩ	f_{peak}/Hz
EL 1	0.51	20	2000
EL 2	0.45	11	1500
EL 3	0.4	8	700
EL 4	0.39	6	500
EL 5	0.29	3.5	400

Note: Z_{max}: the maximum impedance value measured for each electrode; f_{peak}: the peak frequency corresponding to Z_{max}.

Table 4. Fitted values for each electrode in the circuit model

Electrode/ c^{m}2	L/H	C/nF	R_2/Ω	f_{peak}/Hz	Z_{max}/KΩ
EL 1(3.53)	0.6817	10.41	3178	1890	20.60
EL 2(9.82)	0.6839	22.27	2238	1290	13.72
EL 3(16)	0.7719	75.75	1204	659	8.46
EL 4(25)	0.7306	121.50	934.4	534	6.43
EL 5(50)	0.6777	261.30	659.7	378	3.93

Table 5. Pain perception value of subjects by adjusting electrode sizes and different carrier frequencies

Electrode	Perception		Carrier frequency/KHz					MV	SD
			6	7	8	9	10		
EL 1	Readout (Vpp)	subthreshold	8.4	8	9.4	8.4	8	8.44	0.51
		threshold	11	10.4	11	11.2	10.2	10.76	0.39
		suprathreshold	20	20.8	21.6	22	20	20.88	0.82
EL 2	Readout (Vpp)	subthreshold	9.2	9.8	9.2	10	9.2	9.48	0.35
		threshold	11	10	10.6	10	10.5	10.42	0.38
		suprathreshold	15.8	15.6	14.4	13.4	16	15.04	0.99
EL 3	Readout (Vpp)	subthreshold	6.8	6.8	7.68	7.6	6.72	7.12	0.42
		threshold	7.44	7.6	8	8.12	7.12	7.66	0.37
		suprathreshold	9.68	9.68	10.2	9.68	9.84	9.82	0.20
EL 4	Readout (Vpp)	subthreshold	7.12	6.4	7.2	8.12	6.72	7.11	0.58
		threshold	7.92	7.12	7.92	8.6	7.44	7.80	0.50
		suprathreshold	9.68	9.6	10.6	10.7	9.6	10.04	0.50
EL 5	Readout (Vpp)	subthreshold	6.16	5.84	6.4	6.72	7.44	6.51	0.55
		threshold	7.2	6.4	7.12	7.44	7.92	7.22	0.49
		suprathreshold	9.68	10.2	9.52	10.1	9.52	9.8	0.29

Note: Vpp, voltage peak-peak; MV, mean value; SD, standard deviation.

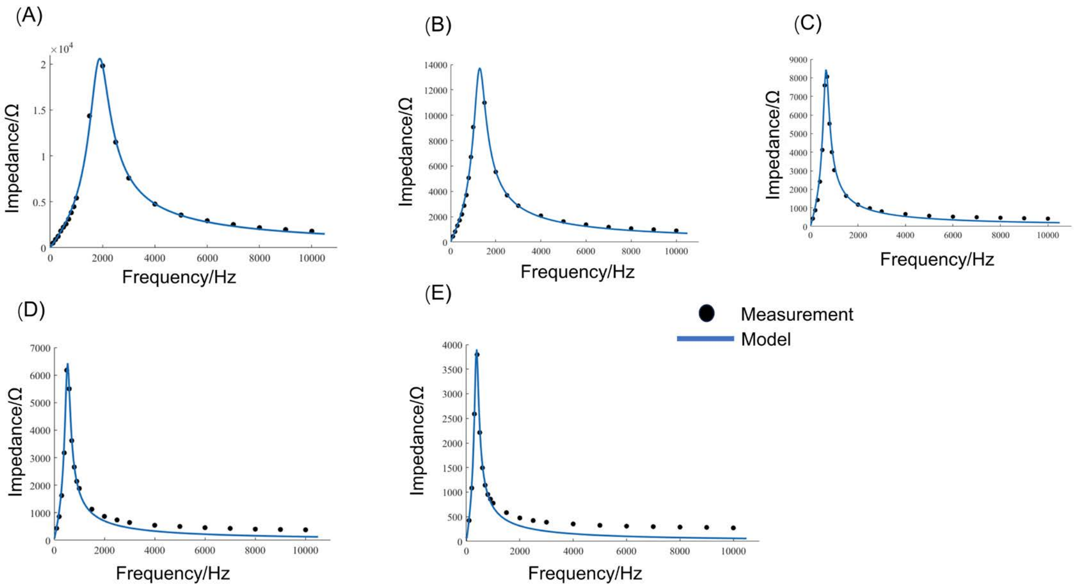

Figure 6. Fitting result of equation (3) for impedance value and its corresponding frequency. The solid dot is the measured data, and the solid line is the fitting curve. (A) Electrode 1; (B) Electrode 2; (C) Electrode 3; (D) Electrode 4; (E) Electrode 5.

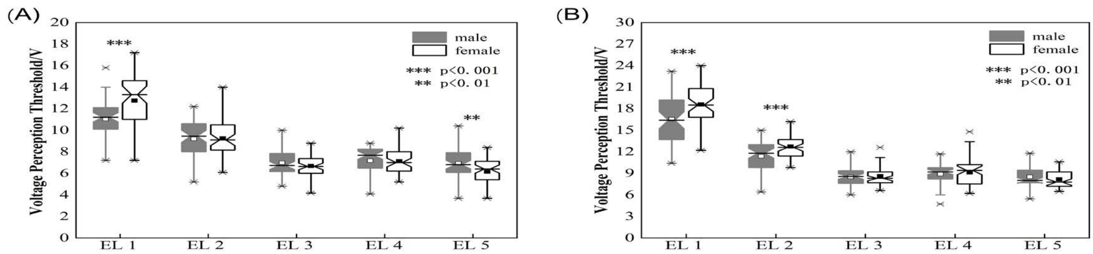

Figure 7. Comparison of the voltage perception threshold obtained from male (gray) and female (white) subjects using five electrodes of different sizes. (A) sensory threshold; (B) supra-sensory threshold. The box plot frames represent the 25th and 75th percentiles, while the whiskers indicate outliers. The small box within the plot represents the mean, the notch indicates the median, and * denotes significant differences between sexes ($^{***}p<0.001$, $^{**}p<0.01$).

threshold measurements, there was no significant difference in VPT values between the 16 cm^2 and 25 cm^2 electrodes. This indicates that the sensation of pain from electrical stimulation is determined by the voltage applied across the electrodes. In traditional electrical stimulation, a constant current source circuit is sued to achieve therapeutic effect by controlling parameters such as current intensity and frequency. However, individuals have different thresholds for current perception, meaning a unified current intensity standard may have different therapeutic effects for different individuals. As a new quantitative standard, VPT value can reflect the pain of electrical stimulation more simply and accurately, thereby achieving a consistent therapeutic effect across different individuals.

Discussion

This study aimed to investigate the maximum impedance of the human body during low-frequency envelope electrical stimulation and determine the appropriate voltage for the power amplifier circuit of electrical stimulation equipment. The measured impedance of the human body depends on the electrode size and the carrier frequency of the output. When using electrode EL1 for electrical stimulation, the impedance range is about 0.4 to 21.6 KΩ. According to **Figure 2a**, achieving a peak output current of 1mA requires a power supply of 216 V, while an output current of 2 mA would require 432 V, and so on. Such high voltage levels are impractical to achieve. The results of the electrical stimulation measurement show that the voltage perceived by the human body is much lower than the above-mentioned power supply value. As shown in **Figure 7**, when the

Table 6. Five common impedance models for human body

Definition	Model	References
Montague	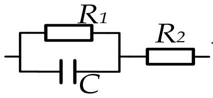 false	[31]
Tregear	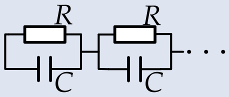 false	[31]
CPE_based	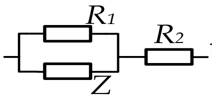 false	[31]
Three-element	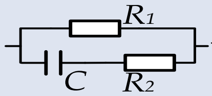 false	[32]
FOIM	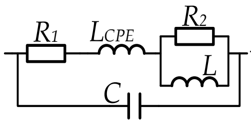 false	[33]

Note: CPE, constant phase element; FOIM, fractional-order impedance models.

VPT exceeds about 10 V, the human body has an obvious sensation of electrical stimulation. The effect of varying electrode sizes is minimal; the sensory threshold ranges from 6-8 V for electrodes of 16 cm2, 25 cm^2 and 50 cm^2, while the supra-sensory threshold ranges from 9 to 11 V.

In addition to differentiating the test subjects by gender, we analyzed the factors affecting the impedance values of the human body using four parameters: different parts of the upper limbs, modulating wave frequency, carrier frequency, and electrode size. Only the electrode size and the output carrier frequency significantly affected the measured value. Notably, the impedance ranges measured by different sizes of electrodes varied significantly. The human impedance circuit model shown in **Figure 6** accurately represents the relationship between carrier frequency and human impedance. Skin impedance model was first developed by Cole, and since then, various impedance models have been proposed [30]. **Table 6** summarizes five common impedance models for the human body [31-33]. The differences in the studies may come from two main factors: 1) Most previous models used single waveform measurement, while this study focuses on the effect of human impedance on electrical stimulation parameters without comparing modulated waveforms to single waveform. 2) This study utilized five different electrode sizes for the measurement of human upper limb impedance, whereas most of the previous studies used a single electrode with unspecified dimensions and inconsistent electrode material. 3) In the previous research, when the frequency range used in the experiment was close to the peak frequency, the relationship between impedance and frequency was typically monotonous - either increasing steadily in the low-frequency range or decreasing steadily in the high-frequency range.

For the measurement of electrical stimulation perception, previous studies have suggested that the factors affecting CPT include current intensity, frequency and electrode size [26]. It is difficult to quantify so many variables. Compared with CPT, the VPT proposed in this study provides a better quantification of pain perception. As shown in **Figure 7**, the sensory threshold and supra-threshold values obtained from electrodes EL3 (electrode), EL4, and EL5 are comparable. The larger differences observed with EL1 and EL2 are due to their sensitivity to the measured values. As shown in **Figure 6**, within the 6-10 kHz range, the impedance values for EL1 and EL2 differ by approximately 1.5 KΩ and 500 Ω, respectively, despite the slower rate of change. This sensitivity is evident in that small currents and frequency changes cause significant voltage changes. While this study does not specifically explore the relationship between human impedance and electrical stimulation perception, the results suggest a positive correlation between these two physiological parameters.

One of the major limitations of this study is that the output intensity of electrical stimulation was not fully measured. Clinically, the output dose of electrical stimulation therapy is typically determined based on the patient's sensory or muscle response [29]. To avoid causing discomfort or pain to the subjects during the experiment, we did not use muscle response as a basis for measuring VPT. In addition, the measurement of human body impedance does not decisively determine the power required for the electrical stimulation power amplifier circuit. The final results show that the output current is not the primary factor affecting the perception of electrical stimulation. Instead, perception is solely related to the voltage across the stimulation site. Regardless of the current output, when the VPT exceeds 10 V, the human body experiences obvious electrical stimulation, which is far less than the product of the current and body impedance. Therefore, this finding suggests a potential shift towards using a constant voltage source circuit instead of constant current source circuit to achieve the desired stimulation effect in future electrical stimulation device. Additionally, we considered whether the inductive characteristic of human upper limb impedance is related to the material of hydrogel electrodes. To verify this, we conducted preliminary experiments with sponge electrodes and observed the same trends, thereby excluding the hydrogel material's influence on impedance values.

In summary, the purpose of this study was to measure the range of human impedance and electrical stimulation sensation to determine the appropriate power supply and output intensity for electrical stimulation devices. The results show that these two parameters should be set based solely on electrical stimulation sensation. A new impedance model proposed in this study accurately fits the measured values. For measuring electrical stimulus perception, this study proposes a new method using the VPT. focuses exclusively on the voltages across the stimulation site, excluding factors such as current intensity and frequency, which significantly simplifies the measurement criteria. Compared to CPT, VPT offers a more precise method for electrical stimulation therapy.

In the next step of the research, the device developed in this study will be refined by adding the voltage detection function to monitor the voltage across the patient's stimulation site in real time. Additionally, the method of measuring the upper limb impedance in this study relies on Ohm's law and collects the voltage at both ends of the electrode, including a part of electrode contact impedance. Future improvements in the measurement method will aim to exclude the influence of electrode contact impedance to provide more accurate results.

Author contributions: Renling Zou and Yuhao Liu are responsible for the overall conception and design of the paper, and put forward the core problems and experimental scheme of the research. Leading the data analysis and the interpretation of experimental results, and writing the main part of the paper, including the introduction and discussion. Yicaiwu, Liang Zhao and Ji Gaodai are responsible for the implementation of the experiment and data collection, participated in the experiment design, and provided suggestions and modifications for some chapters of the paper. Xuezhi Yin assists in the selection and maintenance of equipment and technical platforms used in the research process. Xiufang Hu is responsible for providing materials and financial support for the experiment. This passage helps me translate the following.

References

[1] Gill ML, Grahn PJ, Calvert JS, et al. Neuromodulation of lumbosacral spinal networks enables independent stepping after complete paraplegia. Nat Med 2018;24(11):1677-1682.

[2] Angeli CA, Boakye M, Morton RA, et al. Recovery of Over-Ground Walking after Chronic Motor Complete Spinal Cord Injury. N Engl J Med 2018;379(13):1244-1250.

[3] Rodrigues JC, Avila MA, Driusso P. Transcutaneous electrical nerve stimulation for women with primary dysmenorrhea: Study protocol for a randomized controlled clinical trial with economic evaluation. PLoS One 2021;16(5):e0250111.

[4] Zhou YX, Wang HP, Bao XL, et al. A frequency and pulse-width co-modulation strategy for transcutaneous neuromuscular electrical stimulation based on sEMG time-domain features. J Neural Eng 2016;13(1):016004.

[5] Sanchez B, Pacheck A, Rutkove SB. Guidelines to electrode positioning for human and animal electrical impedance myography research. Sci Rep 2016;6:32615.

[6] Son C, Kim S, Kim S-j, et al. Detection of muscle activation through multi-electrode sensing using electrical stimulation. Sens. Actuators, A 2018;275:19-28.

[7] Sun B, Baidillah MR, Darma PN, et al. Evaluation of the effectiveness of electrical muscle stimulation on human calf muscles via

frequency difference electrical impedance tomography. Physiol Meas 2021;42(3).
[8] Sanchez B, Aroul ALP, Bartolome E, et al. Propagation of Measurement Errors Through Body Composition Equations for Body Impedance Analysis. IEEE Trans Instrum Meas 2014;63(6):1535-1544.
[9] Chinen K, Kinjo I, Zamami A, et al. New equivalent-electrical circuit model and a practical measurement method for human body impedance. Biomed Mater Eng 2015;26 Suppl 1:S779-S786.
[10] Freeborn TJ, Elwakil AS, Maundy B. Compact Wide Frequency Range Fractional-Order Models of Human Body Impedance against Contact Currents. Math Probl Eng 2016;2016(1):4967937.
[11] Demir U, Kocaoğlu S, Akdoğan E. Human impedance parameter estimation using artificial neural network for modelling physiotherapist motion. Biocybern Biomed Eng 2016;36(2):318-326.
[12] Shiffman C. Scaling and the frequency dependence of Nyquist plot maxima of the electrical impedance of the human thigh. Physiol Meas 2017;38(12):2203-2221.
[13] Qiu S, Feng J, Xu R, et al. A Stimulus Artifact Removal Technique for SEMG Signal Processing During Functional Electrical Stimulation. IEEE Trans Biomed Eng 2015;62(8):1959-1968.
[14] Ding JH, Chen ZH, Li YR. Development of functional electrical stimulator with real-time adjustable stimulation parameters. J Fuzhou Univ (Nat Sci Ed) 2019;47(06):759-764.
[15] Yin Q, Li X, Liu Q. [Design of functional array electrode stimulation system with surface electromyography feedback]. Sheng Wu Yi Xue Gong Cheng Xue Za Zhi 2020;37(6):1045-1055.
[16] Zhou Y, Fang Y, Gui K, et al. sEMG Bias-Driven Functional Electrical Stimulation System for Upper-Limb Stroke Rehabilitation. IEEE Sens J 2018;18(16):6812-6821.
[17] van der Lely S, Liechti MD, Bachmann LM, et al. Quantitative electrical pain threshold assessment in the lower urinary tract. Neurourol Urodyn 2020;39(1):420-431.
[18] Seno SI, Shimazu H, Kogure E, et al. Factors Affecting and Adjustments for Sex Differences in Current Perception Threshold With Transcutaneous Electrical Stimulation in Healthy Subjects. Neuromodulation 2019;22(5):573-579.
[19] Oh KJ, Kim SH, Lee YH, et al. Pain-related evoked potential in healthy adults. Ann Rehabil Med 2015;39(1):108-115.
[20] Ji Ri Mu Tu Y, Yin Y, Zhu T. [Determination of electrical stimulation pain perception and analysis of the related factors]. Sheng Wu Yi Xue Gong Cheng Xue Za Zhi 2013;30(6):1200-1203, 1208.
[21] Chang W, Xu W, Hu R, et al. Current Perception Threshold Testing in Pharyngeal Paresthesia Patients with Depression or Anxiety. Neuropsychiatr Dis Treat 2020;16:1023-1029.
[22] Suzuki Y, Muramatsu K, Maruo K, et al. Pain thresholds are unaffected by age in a Japanese population. Muscle Nerve 2020;61(5):653-656.
[23] Solomons CD, Slovak M, Heller B, et al. Reducing the sensation of electrical stimulation with dry electrodes by using an array of constant current sources. Med Eng Phys 2018;51:91-95.
[24] Chan SCC, Peng J, Chan CCH. Reliability of measurements for sub-painful and painful perception on artificial electrical stimulations. Int J Psychophysiol 2018;123:35-41.
[25] Furuse N, Kimoto S, Nakashima Y, et al. Verification of the reliability of current perception threshold and pain threshold testing by application of an electrical current stimulus to mandibular mucosa in young adults. J Oral Rehabil 2019;46(6):556-562.
[26] Hiremath SV, Tyler-Kabara EC, Wheeler JJ, et al. Human perception of electrical stimulation on the surface of somatosensory cortex. PLoS One 2017;12(5):e0176020.
[27] Nitsche MA, Paulus W. Excitability changes induced in the human motor cortex by weak transcranial direct current stimulation. J Physiol 2000;527 Pt 3(Pt 3):633-639.
[28] Reilly JP. Applied bioelectricity: from electrical stimulation to electropathology. USA. Springer New York, NY, 2012.
[29] Shen Y and Zhang ZQ. Clinical work guidelines for rehabilitation therapists - physical factor therapy techniques. Beijing. People’s Health Publishing House, 2019. p. 171-172.
[30] Cole KS and Curtis HJ. Electric impedance of nerve and muscle. Cold Spring Harb Symp Quant Biol 1936;4:73-89.
[31] Bora DJ, Dasgupta R. Estimation of skin impedance models with experimental data and a proposed model for human skin impedance. IET Syst Biol 2020;14(5):230-240.
[32] Rutkove SB. Electrical impedance myography: Background, current state, and future directions. Muscle Nerve 2009;40(6):936-946.
[33] Ghita M, Neckebroek M, Juchem J, et al. Bioimpedance Sensor and Methodology for Acute Pain Monitoring. Sensors (Basel) 2020;20(23):6765.